Binding of 4′,6-Diamidino-2-phenylindole (DAPI) to AT Regions of DNA: Evidence for an Allosteric Conformational Change

Svante Eriksson, Seog K. Kim, Mikael Kubista,* and Bengt Nordén

Department of Physical Chemistry, Chalmers University of Technology, S-412 96 Göteborg, Sweden

Received July 9, 1992; Revised Manuscript Received November 6, 1992

ABSTRACT: The interaction of 4′,6-diamidino-2-phenylindole (DAPI) with several double-helical poly- and oligonucleotides has been studied in solution using optical spectroscopic techniques: flow linear dichroism (LD), induced circular dichroism (CD), and fluorescence spectroscopy. In AT-rich sequences, where DAPI is preferentially bound, LD indicates that the molecule is edgewise inserted into the minor groove at an angle of approximately 45° to the helix axis. This binding geometry is found for very low as well as quite high binding ratios. The concluded geometry is in agreement with that of the DAPI complex in a crystal with the Drew–Dickerson dodecamer, and the DAPI complex with this dodecamer in solution is verified to have an ICD spectrum similar to that of the complex with $[poly(dA–dT)]_2$ at low binding ratios. The observation of two types of CD spectra characteristic for the binding of DAPI to DNA, and also for the interaction with $[poly(dA–dT)]_2$, demonstrates that the first binding mode, despite its low apparent abundance (a few percent), is not due to a specific DNA site. The effect may be explained in terms of an allosteric binding such that when DAPI molecules bind contiguously to the AT sequence the conformation of the latter is changed. The new conformation, which according to LD appears to be stiffer than normal B-form DNA, is responsible for the second type of induced CD spectrum in the DAPI chromophore. Although the spectroscopic results indicate a change of DNA conformation, consistent with an allosteric binding model, they do not explicitly require any cooperativity, but accidental neighbors could also explain the data.

The interaction of DAPI[1] (4′,6-diamidino-2-phenylindole) with DNA has been the subject of numerous studies since this drug was first synthesized (Dann et al., 1971). The original intent was to produce a diamidino compound, analogous to berenil and stilbamidine, to be used as a trypanocide agent. However, the special spectral properties of DAPI have caused it to be used more as a DNA probe. It has been exploited, for example, in electrophoresis (Kapuscinski & Yanagi, 1979; Schwartz & Koval, 1989), for cytofluorometry (Brown & Hitchcook, 1989; Chi et al., 1990; Hajduk, 1976; Lee et al., 1984; Russel et al., 1975; Takato & Hirano, 1990; Tijssen et al., 1982; Williamson & Fennel, 1979) and for staining chromosomes (Bella & Gosálvez, 1991; Bernheim & Miglierina, 1989; Lin et al., 1977).

DAPI forms highly fluorescent complexes with double-stranded DNA (Cavatorta et al., 1985; Kapuscinski & Skoczylas, 1978; Williamson & Fennell, 1975, 1979) with a binding preference for AT-rich regions (Williamson & Fennel, 1975). Footprinting experiments show that a sequence of 3–4 contiguous AT base pairs is covered when DAPI is bound (Jeppesen & Nielsen, 1989; Portugal & Waring, 1988). Different techniques such as fluorescence (Härd et al., 1990; Lin et al., 1977), linear dichroism (Kubista et al., 1987), NMR (Wilson et al., 1990), and viscometry (Manzini et al., 1985) suggest that DAPI is located in the minor groove of the DNA helix in this high-affinity binding mode. A detailed description of the geometry of this complex between DAPI and DNA is provided from the crystal structure of DAPI bound to the dodecamer, $[d(CGCGAATTCGCG)]_2$, where it is found in the minor groove of the central AATT sequence (Larsen et al., 1989).

Most studies have concerned this high-affinity binding mode, but heterogeneity in the binding has been evidenced at higher binding ratios both with DNA and with some polynucleotides (Bierzynski et al., 1978; Kapuscinski & Szer, 1979; Kubista et al., 1987; Manzini et al., 1983, 1985; Nordén et al., 1990; Wilson et al., 1990). Several explanations have been put forward, including an allosteric change of the DNA structure (Nordén et al., 1990; Wilson et al., 1990). Wilson and co-workers (1989) have shown that DAPI can bind to GC sequences too, possibly by an intercalative binding mode.

The structural interpretation of spectroscopic data of DAPI–DNA complexes requires knowledge of the basic electronic properties of the ligand chromophore. The broad near-UV absorption of DAPI originates from two electronic transitions; one is dominating the long wavelength region and is polarized along the molecular long axis of DAPI, and one at slightly shorter wavelength is polarized some 15° to the former (Kubista et al. 1989). In aqueous solution their absorption maxima are centered around 363 and 334 nm, respectively. The two transitions involve both the indole and the phenol chromophores (Albinsson et al., 1991). The photophysics of DAPI is complex, probably involving both ground-state and excited-state heterogeneities (Barcellona & Gratton, 1990, 1991). The large increase in the fluorescence quantum yield of DAPI upon binding to AT regions has been attributed to hindrance of an intramolecular proton transfer in the excited state, which in solution gives rise to rapid quenching of the fluorescence (Szabo et al., 1986).

* Author to whom correspondence should be addressed.

[1] Abbreviations: A, adenine; C, cytidine; CD, circular dichroism; DAPI, 4′,6-diamidino-2-phenylindole; DNA, deoxyribonucleic acid; EDTA, ethylenediaminetetraacetic acid; G, guanine; LD, linear dichroism; LD^r, reduced linear dichroism; $[poly(dA–dT)]_2$, duplex of alternating poly(dA–dT); $[poly(dG–dC)]_2$, duplex of alternating poly(dG–dC); T, thymine; Tris, tris(hydroxymethyl)aminomethane; λ, wavelength.

0006-2960/93/0432-2987$04.00/0

Despite extensive studies of DAPI's interaction with DNA, a number of questions have remained unanswered concerning the geometrical prerequisites for its binding, i.e., the sequence dependence, and how the geometries differ between various modes of binding. The objectives of this study are to characterize the different DNA binding modes of DAPI with respect to structure and to study how already bound DAPI molecules may influence additional binding. Spectroscopic data (circular and linear dichroism, absorption, and fluorescence) are presented for DAPI complexes, at various binding ratios, with [poly(dA–dT)]$_2$ and with a few oligonucleotides designed to address some specific questions regarding the binding.

Our results are consistent with a model in which DAPI binds cooperatively to the minor groove of [poly(dA–dT)]$_2$ and in which the binding of several drug units leads to a conformational change of the polynucleotide. At high degrees of occupancy, crowding in the groove leads to the exciton type of interactions between adjacent DAPI molecules. The spectral features of the DAPI complexes with the dodecamer [d(CGCGAATTCGCG)]$_2$ (also studied as a crystal), the alternating AT duplex, and natural DNA are very similar at low binding ratios, confirming similar minor groove binding in all of these cases. In addition, the binding of DAPI to oligonucleotides containing AT sequences of varying lengths indicates that sequences longer than four AT base pairs give a cooperative behavior while a short run of four AT base pairs behaves like a single site, in agreement with recently reported data on a decamer (Loontiens et al., 1991).

MATERIALS AND METHODS

Chemicals. [poly(dA–dT)]$_2$ was obtained from Pharmacia, and the oligonucleotides were synthesized on an Applied Biosystems 381A DNA synthesizer and purified by FPLC. The purity of the oligonucleotides was in most cases checked by electrophoresis. DAPI was purchased from Serva and was used without further purification. All concentrations were determined spectrophotometrically using the following molar absorption coefficients: $\epsilon_{262} = 6600\ M^{-1}\ cm^{-1}$ for [poly(dA–dT)]$_2$; $\epsilon_{342} = 27\,000\ M^{-1}\ cm^{-1}$ for DAPI in water (Kapuscinski & Skozylas, 1978). For all synthetic oligomers, the same value of $\epsilon_{260} = 6600\ M^{-1}\ cm^{-1}$ was used, which we estimate to give correct concentrations within 10%. All nucleic acid concentrations are expressed in nucleotide bases, and oligomer sequences are presented as 5′ → 3′.

The mixing ratio, R, is defined as the total number of added DAPI molecules per nucleotide base (for the polynucleotides) alternatively per oligomer. It may deviate somewhat from the binding ratio, which is the number of bound DAPI molecules per base. However, since the binding of DAPI to AT sequences is very strong at low ionic strength, R is essentially equal to the true binding ratio under our conditions (10 mM Tris), even at relatively high mixing ratios. Reported association constant in 100 mM NaCl is $2.9 \times 10^7\ M^{-1}$ with [poly(dA–dT)]$_2$ (Loontiens et al., 1991). As confirmed from the absorption spectra, the amount of free DAPI did not in any case exceed 20% and was in most cases far below this level.

Unless otherwise stated, the experiments were conducted in 10 mM Tris and 1 mM EDTA (pH 7.4). Measurements with the oligonucleotides were performed at 2–3 °C to minimize strand separation, and measurements with long DNA were made at room temperature.

Linear dichroism (LD) is defined as

$$LD(\lambda) = A_{\parallel}(\lambda) - A_{\perp}(\lambda) \quad (1)$$

where $A_{\parallel}(\lambda)$ and $A_{\perp}(\lambda)$ are the absorption spectra measured with the light plane polarized parallel and perpendicular, respectively, to the flow direction in a Couette cell with light propagating radially through the two concentric silica cylinders (Nordén et al., 1992). The LD data are evaluated as the *reduced linear dichroism*, LD^r, defined as

$$LD^r(\lambda) = LD(\lambda)/A_{iso}(\lambda) \quad (2)$$

where $A_{iso}(\lambda)$ is the absorption spectrum for the isotropic sample in the absence of flow. This dimensionless quantity is related to the orientation of the light-absorbing transition moment as

$$LD^r = SO = S\left(3\,\frac{3\langle\cos^2\alpha\rangle - 1}{2}\right) \quad (3)$$

where S is an orientation factor describing the degree of orientation of the DNA helix in the gradient shear. It depends on the stiffness of the DNA, the flow rate, and the viscosity of the medium (Nordén et al., 1992). The optical factor, O, reflects the angle, α, between the transition moment of absorption and the local DNA helix, and the brackets denote an ensemble average over the angular distribution. When several transitions are involved, the measured LD^r will be an average of the LD^r values of the individual transitions weighted with their respective absorbances. The $\pi \rightarrow \pi^*$ transitions of the DNA bases, which are responsible for the LD of the polynucleotide around 260 nm, are polarized in the plane of the bases with an effective angle, $\alpha = 86°$, between the planes of the bases and the helix axis (Matsuoka & Nordén, 1982, 1983). This angle is used to calculate the orientation factor, S, from the measured LD^r of the DNA bases. The LD spectra were measured on a Jasco J-500 spectropolarimeter as described elsewhere (Nordén & Seth, 1985).

Circular dichroism is the differential absorption of circularly polarized light:

$$CD(\lambda) = A_l(\lambda) - A_r(\lambda) \quad (4)$$

where A_l and A_r are the absorbances measured with left and right circularly polarized light. DAPI itself is not chiral but acquires CD when bound to the chiral DNA. The mechanism behind this induced CD is not clear in detail but is believed to be an effect of nondegenerate coupling between transitions of DAPI and transitions of the bases of the nucleic acid host (Kubista et al., 1989; Lyng et al., 1991). All CD spectra were measured on the Jasco J-500 spectropolarimeter using a 1-cm quartz cell.

Absorption spectra were recorded on a Varian Cary 2300 spectrophotometer and *fluorescence spectra* on an Aminco SPF-500 spectrofluorometer in the quantum-corrected mode. All spectra were corrected for the inner filter effect.

Normalization. The titrations were made either at constant DAPI concentrations or at constant nucleotide concentrations, but the presented data (except for LD) have been normalized with respect to the (total) DAPI concentration.

RESULTS

[poly(dA–dT)]$_2$

LD at Low Binding Ratios. Figure 1a–c shows the linear dichroism, as well as the absorption and the calculated reduced linear dichroism, at various DAPI/DNA mixing ratios. The

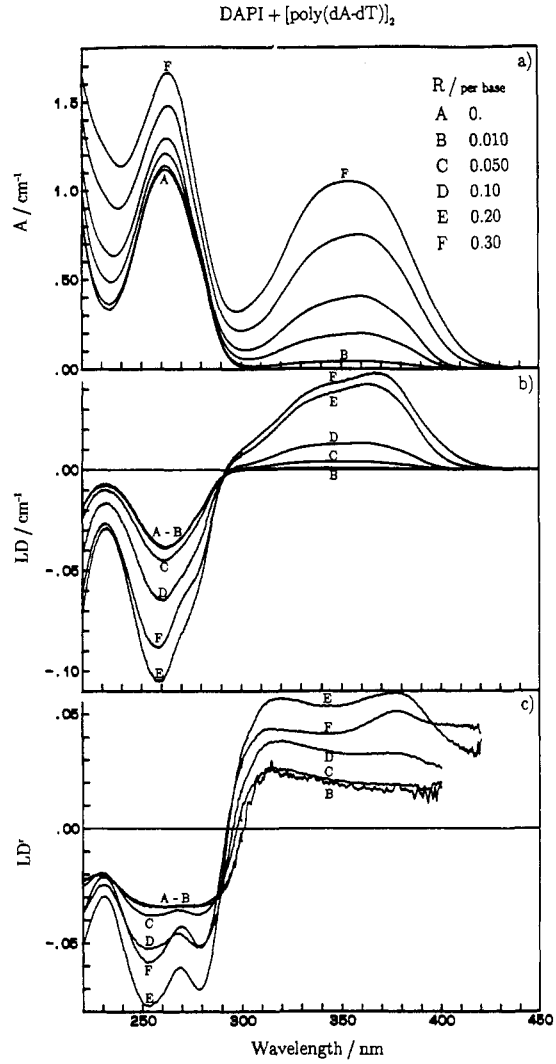

FIGURE 1: Absorption (A), linear dichroism (LD), and reduced linear dichroism (LD^r) of DAPI in the presence of $[poly(dA–dT)]_2$ at various DAPI per DNA base mixing ratios (R).

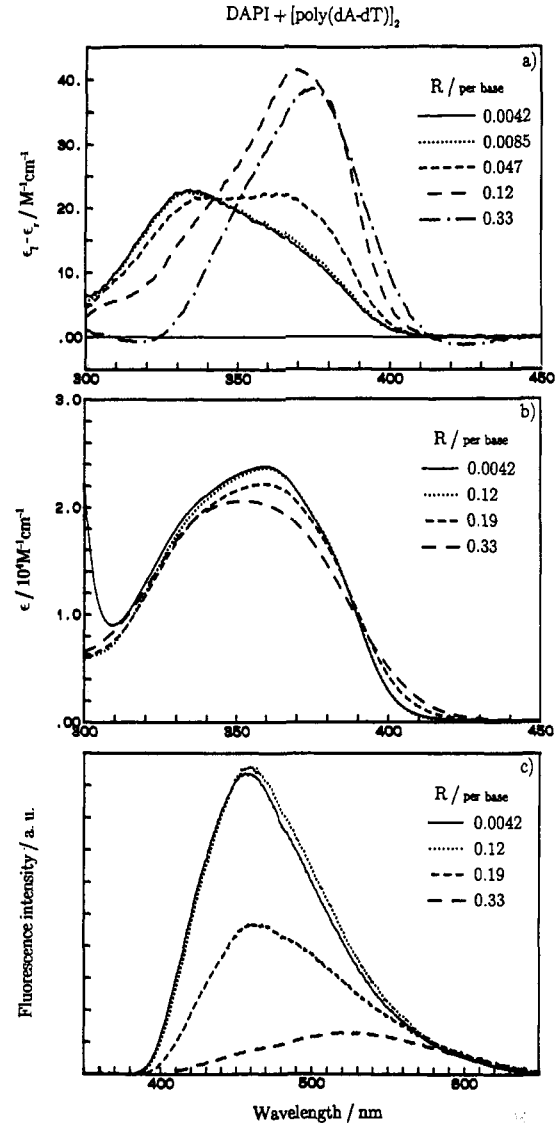

FIGURE 2: Circular dichroism ($\epsilon_l - \epsilon_r O$), absorption coefficient (ϵ), and fluorescence of DAPI and $[poly(dA–dT)]_2$ at various DAPI per DNA base mixing ratios (R). Data normalized to unit DAPI concentration.

LD is negative for the polynucleotide in the $\pi \rightarrow \pi^*$ transition region around 260 nm, in accord with the planes of the bases in B-DNA being perpendicular to the helix axis. For DAPI the LD is positive in the 300–400-nm region, where DAPI is known to have two electronic transitions polarized near the long axis of the molecule (Kubista et al., 1989). With the orientation factor S calculated from the reduced dichroism of the DNA absorption band at 260 nm, the LD^r of DAPI gives an effective angle α of 43–46°, varying slightly from the long to the short wavelength end of the absorption region 300–400 nm. The contribution from DAPI at 260 nm is negligible compared to the nucleic acid absorption at low binding ratios. The orientation of DAPI with the alternating AT duplex is essentially the same as that concluded with calf thymus DNA at a low binding ratio (Kubista et al., 1987). According to a crystal study of DAPI bound to an oligonucleotide, the tile angle is 45° (Larsen et al., 1989), which agrees very well with our results.

LD at High Binding Ratios. As more and more DAPI binds to the polynucleotide, the orientation factor S increases as judged from the increase of $|LD^r|$ for DNA at 260 nm, as well as for the DAPI band at $\lambda > 300$ nm. The binding of DAPI at these higher ratios thus seems to lead to a stiffening and/or a lengthening of the polynucleotide. A virtual change in shape of the LD^r spectrum of DAPI at $\lambda > 300$ nm at the highest mixing ratios is mainly a result of the presence of some free DAPI, which does not contribute to the LD but contributes to the absorption in the calculation of LD^r (cf. eq 2). A similar decrease of the LD signal also occurs at 270 nm and can be attributed to the presence of free DAPI, but it is in part also due to absorption from bound DAPI. The orientation of DAPI relative to the DNA helix axis thus seems to be essentially independent of the binding ratio.

CD at Low and Intermediate Binding Ratios. While the LD spectra reveal no significant difference in the orientation of DAPI between low and intermediate binding ratios, the CD spectra show marked variations (Figure 2a). At very low binding ratios, the DAPI CD spectrum induced by the presence of the polynucleotide consists of a positive feature with a maximum at 335 nm. An identical spectrum is observed when DAPI binds to natural DNA at very low ratios, and it has been denoted as the "type I spectrum" (Manzini et al., 1983). However, at $R = 0.02$, corresponding to one DAPI per 50 bases, a new and more intense induced CD band already appears with a maximum at 375 nm, providing evidence for the presence of a component denoted as the "type II spectrum". The spectral transition displays an isosbestic point at 341 nm. It should be noted that no corresponding structural change is evidenced by any other spectroscopic technique at these low

binding ratios. Clearly, CD is more sensitive to variations in binding geometry than the other spectroscopic properties and is able to detect structural changes associated with multiple binding.

CD at High Binding Ratios. As R increases to about 0.15, a new (negative) CD feature builds up at $\lambda > 400$ nm. This feature has its counterpart in changes in absorption and fluorescence (see below) and is characteristic for strong electronic interactions between the ligands. We interpret it as an exciton type of interaction between DAPI molecules forced to be bound close to each other due to crowding on the polynucleotide substrate.

Absorption. Figure 2b shows the absorption spectra of free and bound DAPI. The binding of DAPI to the polynucleotide is accompanied by a hypochroism of about 12% and a red shift of the absorption maximum above 300 nm by about 20 nm. These features remain constant up to a binding ratio of 0.12, i.e., within the range where large changes are observed in the CD spectra. At higher mixing ratios, however, the absorption decreases drastically and shifts to even longer wavelengths as a result of the mentioned DAPI–DAPI interactions.

Fluorescence. There is a large increase in the quantum yield and a narrowing of the shape of the emission spectrum when DAPI binds to [poly(dA–dT)]$_2$ (Figure 2c). As with the absorption, the fluorescence intensity is constant up to $R = 0.12$. At higher ratios the emission decreases significantly and shifts to longer wavelengths. Again this behavior is consistent with exciton interactions between closely bound DAPI molecules.

From these results we conclude that DAPI binds to [poly(dA–dT)]$_2$ in two different modes, the "AT mode I" and the "AT mode II". The two binding modes are directly related to the type I and type II CD spectra, respectively. For both binding modes DAPI is bound with its long axis at about 45° to the polynucleotide axis. In the AT mode I, DAPI molecules are bound isolated, whereas the AT mode II requires the presence of previously bound DAPI molecules, which results in a higher binding affinity and a stiffening of the DNA fiber. At very high mixing ratios we see evidence of Coloumbic (exciton) interactions between bound DAPI molecules.

[*d(ATATATATATAT)*]$_2$

CD. The magnitude of the induced CD of DAPI bound to the AT dodecamer is some 40% smaller than the CD of DAPI bound to [poly(dA–dT)]$_2$, and the spectral shape is somewhat different (Figure 3a). These differences can most likely be ascribed to the short length of the oligomer and to fraying of the ends, since the strength of the induced CD depends on the length of the duplex substrate (Kubista et al., 1989; Lyng et al., 1991). The principal behavior of the oligomer is similar, however, to that of the AT polymer: the CD of the bound DAPI changes gradually from a type I to a type II spectrum, evidencing initial binding in AT mode I and subsequent binding in AT mode II. The change of binding mode is already readily observed at low binding ratios, as expected for cooperative binding. For example, at a mixing ratio of one DAPI per oligomer, the recorded CD spectrum has a clear type II character, meaning that a considerable amount of the DAPI molecules are bound in AT mode II. Since the AT mode II requires the presence of more than one DAPI molecule per oligomer, the bound DAPI molecules must be unevenly distributed among the oligomers, as is expected for cooperative binding. At even higher mixing ratios (more than two DAPI molecules per oligomer) a negative CD feature appears at long wavelengths, evidencing exciton interactions between bound DAPI molecules.

Absorption and Fluorescence. The binding of DAPI to the AT dodecamer is accompanied by a decrease of about 20%, a red shift of some 20 nm of the absorption spectrum (Figure 3b), and a 40-fold increase in fluorescence intensity (Figure 3c). These changes are comparable to those observed upon binding of DAPI to [poly(dA–dT)]$_2$, suggesting similar modes of interaction. These features remain constant up to a mixing ratio of two DAPI molecules per oligomer, whereafter a decrease and red shift of both absorption and fluorescence intensity are seen, evidencing exciton interactions between bound DAPI molecules.

[*d(ATATAT)*]$_2$

CD. With the AT hexamer the CD titration turned out differently (Figure 3d). At the lowest binding ratio the CD spectrum is close to a type I spectrum, but there is no conversion into a type II spectrum as the mixing ratio is increased. Instead, there is a negative feature at 400 nm, reflecting exciton interactions between DAPI molecules and showing that more than one DAPI molecule can bind to the hexamer. This oligomer is apparently too short to promote cooperative binding to AT mode II, which evidently requires at least two bound units possibly at a certain minimum distance from each other.

Absorption. The absorption spectrum of the singly bound DAPI molecules is not identically the same as that with the longer AT oligo- and polynucleotides (Figure 3e). The hypochromism is similar, about 20%, but the red shift is less, about 10 nm, and the spectral shape is somewhat changed. This could be an effect of the fact that the hexamer is too short to be completely in duplex form and/or that the end effects are large. Indeed, a small decrease of the absorption, by a few percent, is observed in the DNA absorption band at 260 nm when DAPI is added to the oligomer solution (results not shown). This can be understood as a shift of the equilibrium between single- and double-stranded oligonucleotides due to a stabilization of the duplex as DAPI binds. Such a stabilization is also evidenced from a nearly 40 °C elevation of the melting temperature of [poly(dA–dT)]$_2$ upon binding of DAPI (data not shown).

Fluorescence. The fluorescence emission increases upon binding just as with the dodecamer, but a decrease, and a slight red shift, with increasing R is observed for the entire interval studied (Figure 3f).

[*d(CGCGAATTCGCG)*]$_2$, [*d(CGCGATATCGCG)*]$_2$, *and* [*d(GCATATGC)*]$_2$

CD. Up to a mixing ratio of one DAPI per oligomer, the shapes of the CD spectra of DAPI bound to the dodecamers [d(CGCGAATTCGCG)]$_2$ (the Drew–Dickerson dodecamer) (Figure 4a) and [d(CGCGATATCGCG)]$_2$ (Figure 4b), as well as to the octamer [d(CGATATGC)]$_2$ (Figure 4e), are all very similar to that of DAPI bound to [poly(dA–dT)]$_2$ at a low degree of occupancy. Only the strength of the CD is weaker by nearly a factor of 2. The constancy in shape demonstrates that there is no cooperative binding to these oligonucleotides. As R increases above one DAPI per oligomer, a negative dip at 400 nm appears, implying interaction between bound DAPI molecules. Whether the increase in CD around 370 nm is due to exciton interaction alone or whether mode II binding is also possible to these oligomers, despite the short AT sequence, is not possible to settle. Binding to the GC sequences may also be anticipated, but the CD from such complexes should be relatively weak

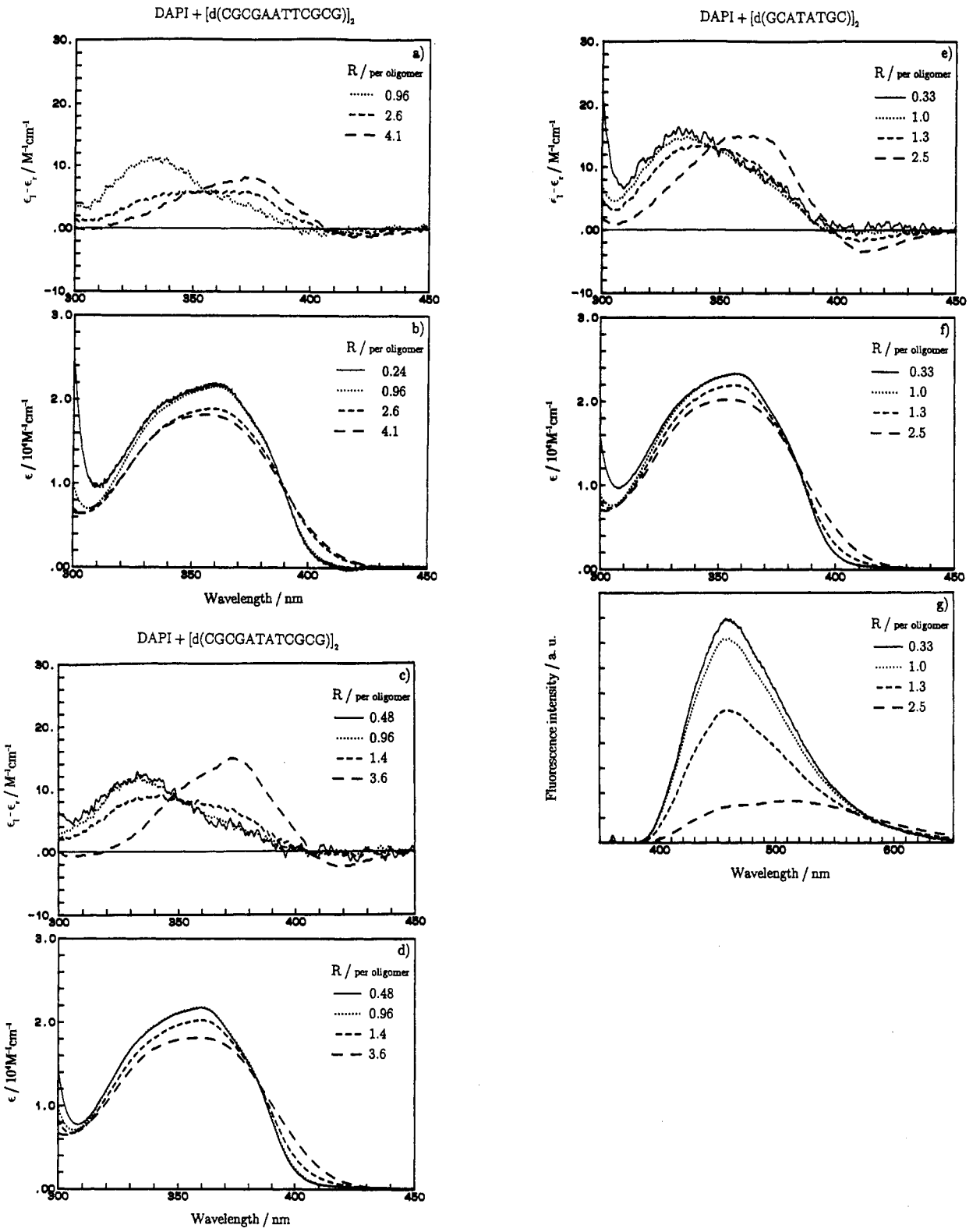

FIGURE 3: Circular dichroism ($\epsilon_l - \epsilon_r$), molar absorptivity (ϵ), and fluorescence of DAPI and [d(CGCGAATTCGCG)]$_2$ (a, b), [d(CGCGATATCGCG)]$_2$ (c, d), and [d(GCATATGC)]$_2$ (e–g) at various DAPI per oligomer duplex mixing ratios (R). Data normalized to unit DAPI concentration.

as judged from the CD of DAPI bound to [poly(dG–dC)]$_2$ (Nordén et al., 1990). According to the CD behavior, as many as 3–4 DAPI molecules can bind to each dodecamer, and at least two DAPI molecules can bind to the octamer.

Absorption. The shapes of the absorption spectra of DAPI when bound to the oligomers at low ratios are similar to that of the complex with [poly(dA–dT)]$_2$, but with absorptivities that are somewhat smaller (Figure 3b,d,f). With more than one DAPI bound per oligomer molecule the absorption is further decreased and shifted toward longer wavelength as a result of exciton interactions between adjacent DAPI molecules.

Fluorescence. DAPI bound to the octamer displays a 30-fold increase in fluorescence emission intensity and a narrowing of the spectrum (Figure 4g). As R approaches one DAPI per oligomer, the intensity starts to decrease and a new emission

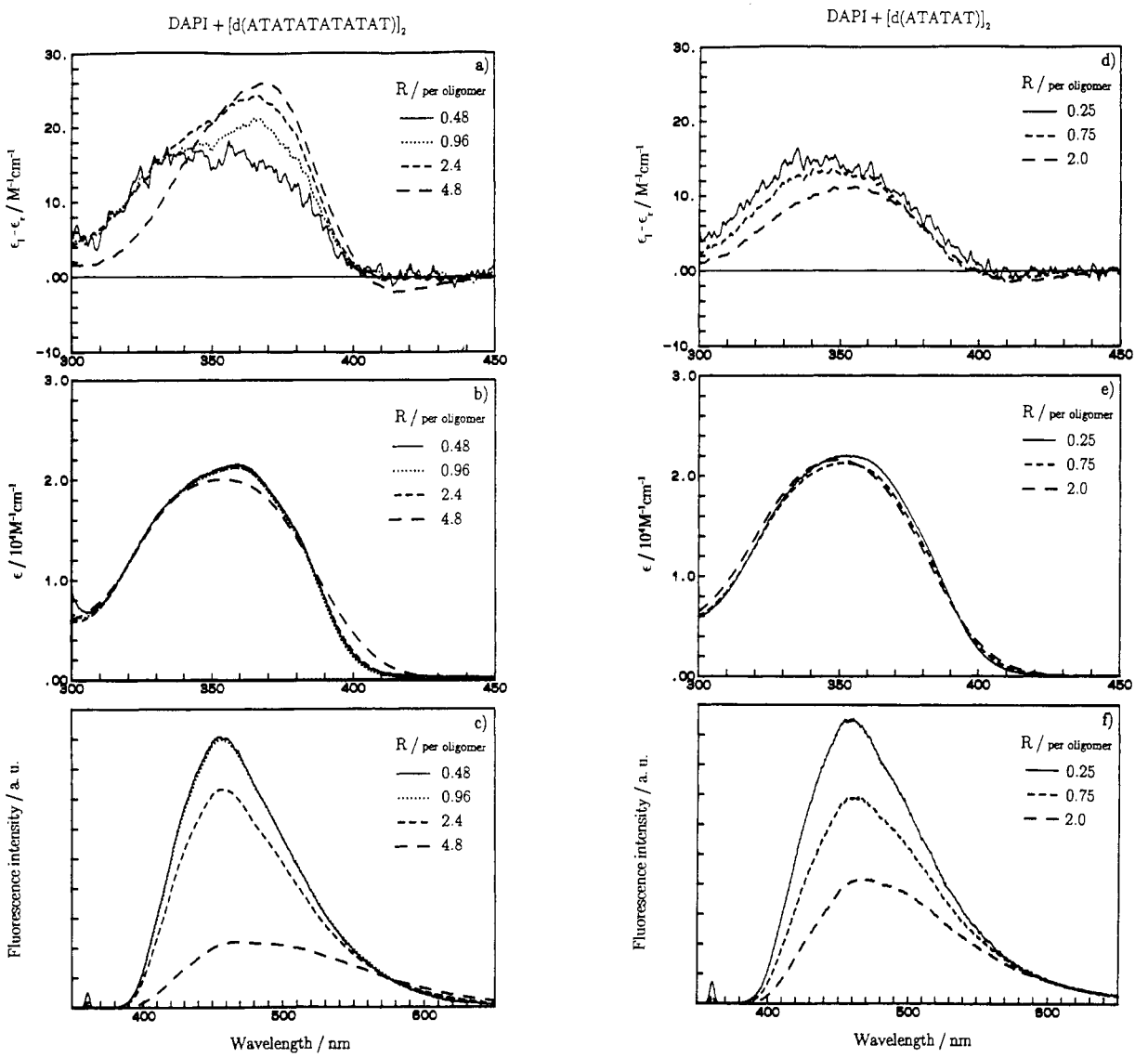

FIGURE 4: Circular dichroism ($\epsilon_l - \epsilon_r$), molar absorptivity (ϵ), and fluorescence of DAPI and [d(ATATATATATAT)]$_2$ (a–c) and [d(ATATAT)]$_2$ (d–f) at various DAPI per oligomer duplex mixing ratios (R). Data normalized to unit DAPI concentration.

arises at lower wavelengths, again demonstrating interactions between DAPI chromophores that are bound on the same oligonucleotide.

DISCUSSION

In this work, we address a number of questions regarding the details of the binding of the dye 4′,6-diamidino-2-phenylindole to DNA. It is clear from our results that the binding mode depends on the binding stoichiometry as well as on the DNA sequence, in agreement with the findings by Wilson et al. (1990). Our findings suggest, as will be discussed below, how a ligand, when bound contiguously to DNA, can induce alterations of the DNA structure. As a model system DAPI may provide insight important for the understanding of potential long-range actions in DNA–drug and DNA–protein complexes in vivo.

Binding of DAPI to AT Regions. A problem in early studies of the binding of DAPI to DNA has been the interpretation of the "second binding site", evidenced from changes in the circular dichroism spectrum at binding ratios around 0.02 in DNA. A crucial finding is the observation that a homopolynucleotide, [poly(dA–dT)]$_2$, also shows the same behavior, demonstrating that the virtual low abundancy of the first site is not due to any specific sequence of DNA. We shall argue that the second site is a conformational effect due to an allosteric binding of DAPI in the minor groove. This hypothesis (Nordén et al., 1990) has support in binding isotherm studies which are consistent with a strongly cooperative binding of DAPI to [poly(dA–dT)]$_2$ (Wilson et al., 1990).

The flow linear dichroism results (Figure 1a–c) show that DAPI bound to [poly(dA–dT)]$_2$ is oriented with its long axis polarized transitions at an angle of 43–46° relative to the helix axis. The constant LD^r over the 320–400-nm region is consistent with a near-planar DAPI conformation in the complex. This angular orientation is in good agreement with the crystal structure of the DAPI complex with [d(GCG-CAATTCGCG)]$_2$, where DAPI is sitting edgewise inserted into the minor groove at 45° to the helix axis (Larsen et al., 1990).

That the drug is residing deep in the groove is evidenced by the observation of a complete protection against quenching of the fluorescence by iodine (S. K. Kim et al., unpublished results) as well as by iodide ion (Nordén et al., 1990). Additional evidence that the binding geometry of DAPI in [poly(dA–dT)]$_2$ is very similar to that found in the crystal is

our observation of almost identical induced circular dichroism spectra of DAPI when bound to this polynucleotide and to the oligomer used in the crystal study. We also note that the same CD spectra are observed when DAPI is bound to the oligonucleotides $[d(CGCGATATCGCG)]_2$ and $[d(GCATATGC)]_2$ at stoichiometries below one drug molecule per oligonucleotide. In other words, the same type of minor groove binding geometry is found whether DAPI is bound to an ATAT or to an AATT sequence.

Wih increasing binding ratios, neither of the AT-type DAPI complexes exhibits any major change in binding geometry. In $[poly(dA–dT)]_2$ DAPI is, according to linear dichroism, bound at an angle of about 45°, consistent with minor groove binding and independent of binding ratio. Also the absorption and emission features indicate that there are no significant variations in the binding mode. By way of contrast, strong variations in circular dichroism clearly demonstrate that some changes occur. The fact that the CD changes are observed already at rather low mixing ratios gives an indication that they may not be due to interactions between bound species that are accidentally close to each other but that this is more likely to be a cooperative phenomenon. A convex binding isotherm has been reported by Wilson et al. (1990) for DAPI with $[poly(dA–dT)]_2$, consistent with cooperative or allosteric binding. Furthermore, the appearance of a type II CD, which is not accompanied by corresponding changes in the absorption and fluorescence spectra, may indicate that the type II is not due to the different molecular conformation itself. The different conformations of DAPI would interact with DNA in different ways; hence, the changes in the absorption and fluorescence spectrum would be expected. We may explain the notable CD behavior in such terms as follows.

Binding Model for Cooperative Allosteric Binding of DAPI to AT Regions. Figure 5 schematically shows three possible simplistic models for cooperative binding. Model A, which does not involve any structural change of the DNA lattice, assumes that the extra binding affinity for a second DAPI molecule stems from attractive interactions between the two bound ligands. However, the DAPI molecules carry a divalent positive charge and should repell each other electrostatically. Further, if the DAPI molecules had been closely interacting with each other, their electronic structures should have been perturbed, and this would have been revealed by changes in the absorption and fluorescence spectra. Indeed, spectral changes evidencing Coulombic (exciton) interactions between bound ligands are observed, however, first at very high binding ratios, far beyond those for the AT mode II binding. We therefore discard scheme A as important for any cooperative binding of DAPI to $[poly(dA–dT)]_2$.

In model B, the binding of the first DAPI molecule is assumed to induce some conformational change of the DNA lattice, with the result that the additional DAPI will bind with somewhat greater affinity. In this scheme all DAPI molecules, both those bound isolated and those bound cintiguously, sit on the same, perturbed lattice. This scheme can also be discarded, since isolated and contiguous DAPI molecules are bound differently as evidenced from their distinctly different CD spectra.

In model C the isolated DAPI molecules bind to an unperturbed lattice, but when bound contiguously they induce some conformational change of the lattice which is favorable for binding and gives a greater affinity. Note that in this scheme, the isolated DAPI molecule is bound in the AT mode I; however, when additional DAPI molecules bind contiguously, the ligands become bound in the AT mode II, in agreement with our results. How extensive this allosteric change of the DNA structure is cannot be deduced solely from our results. No significant change of the orientation of DAPI is seen, indicating that the helicity and pitch of the duplex are effectively retained. On the other hand, the large increase of the LD^r of the polymer shows that the binding leads to a considerable stiffening of the structure, which might be related to such an allosteric conformational change, but which also might be an effect of DAPI filling the minor groove and decreasing the bendability of DNA.

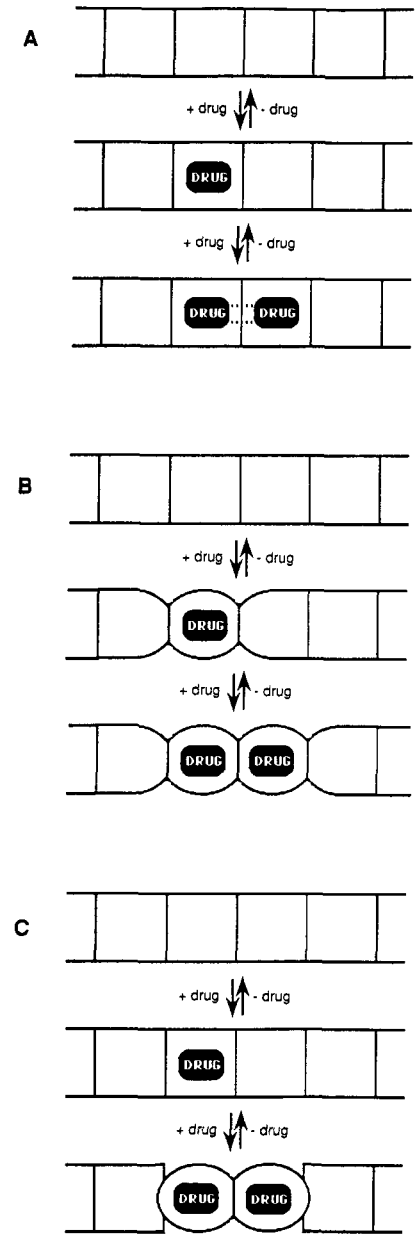

FIGURE 5: Three models for cooperative binding (see text for explanation).

The CD spectra of DAPI bound to $[poly(dA–dT)]_2$ (Figure 6a) were analyzed using a chemometric approach (see Appendix 1), allowing an estimate of the pure spectrum of the induced CD of DAPI in the AT mode II and the amount of DAPI bound in the two modes at different binding ratios. The type II CD spectrum can be deduced only within certain limits (see Appendix 1 for an explanation), and in Figure 6 two cases are depicted. A criteron for Figure 6d,e was that the analysis should produce a mode II spectrum that has reasonable shape and intensity. As seen in Figure 6e, the amount of

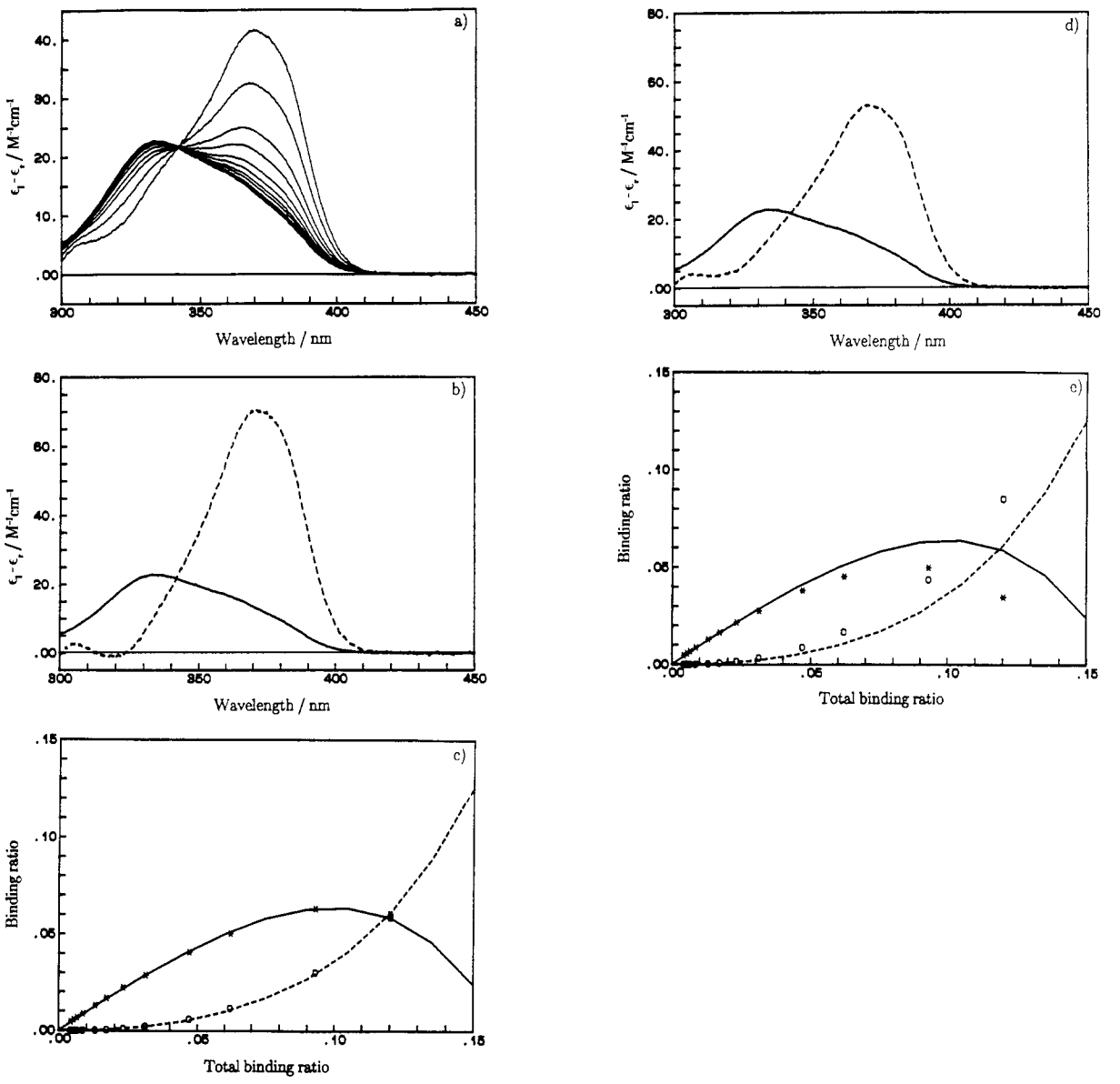

FIGURE 6: CD spectra of DAPI bound to [poly(dA–dT)]$_2$ after noise reduction by chemometric treatment (a). CD spectra of DAPI bound in mode I (—) and mode II (- - -) (b). Corresponding binding isotherms for mode I (*) and mode II (O) calculated by chemometry compared to binding isotherms for random occurrence of isolated DAPI molecules (—) and DAPI molecules with at least one neighbor (- - -) (c). The R_{11} parameter, and thereby the mode II spectrum, was tuned to give best fit of CD data to the case of random binding. Another possible solution by the chemometric approach where R_{11} is tuned to give an all-positive mode II CD spectrum with a physically reasonable shape (d, e). Here, the calculated binding isotherms predict a larger occurrence of contiguously bound DAPI ligands than expected from random association.

DAPI in AT mode I initially increases linearly with increasing total amount of bound DAPI and reaches a maximum at about 0.09 DAPI molecule per DNA base. The amount of DAPI in the AT mode II is initially very low but increases roughly quadratically with the amount of DAPI added. The binding isotherms indicate that molecules initially bound in the AT mode I are converted into the AT mode II as the titration proceeds, as predicted by scheme C. (The thermodynamics of the allosteric binding is discussed in more detail in Appendix 2.) Allowing that a mode II peak is somewhat larger, but definitely not unphysical, gives a perfect match between the two modes of binding and the occurrence of isolated ligands and ligands with at least one neighbor, as calculated by the model of McGhee and von Hippel (1974) assuming no cooperativity (Figure 6b,c). The chemometric analysis cannot unambiguously point out a binding mechanism but can at least hint at a possible solution. We see that cooperative binding and accidental neighbors are both possible.

Binding of DAPI to Oligonucleotides. Let us see how this model applies to the interpretation of binding of DAPI to the oligonucleotides. For the AT dodecamer, just as with [poly(dA–dT)]$_2$, increasing binding ratio leads to a type II CD spectrum with a positive maximum around 375 nm. The change in CD is observed at a binding ratio of much less than one drug per oligonucleotide, which is consistent with a cooperative binding. The dodecamers [d(CGCGAATTCGCG)]$_2$ and [d(CGCGATATCGCG)]$_2$ both show, at low binding ratios, a CD feature characteristic of mode I, and at higher binding ratios, there is evidence for a second mode of binding. However, in these cases no cooperativity is observed, but the "switching point" occurs around one drug molecule bound per oligonucleotide unit. The same holds for the octamer [d(GCATATGC)]$_2$.

The different behavior in the shorter AT tracts can be viewed as an effect of two DAPI molecules being forced to bind more closely together, thereby losing some of the free energy of

binding due to mutual electrostatic repulsion by their divalent cationic charge. Indeed, the appearance of an exciton type of interaction of circular dichroism at low binding ratios, as well as corresponding changes in absorption and fluorescence, shows that the two DAPI molecules are closer than in the longer AT tract complexes at a corresponding binding ratio. This observation provides an important corollary as to the minimum size of the drug–drug distance in the normal "dimeric" type II binding mode where no such interactions are observed.

Exciton Interaction. In the absorption, linear and circular dichroism, and fluorescence spectra of the binding of DAPI to [poly(dA–dT)]$_2$ and the AT-containing oligonucleotides, there is evidence for electronic (exciton) interactions between adjacent DAPI molecules at high binding ratios. The LD spectrum of the DAPI–[poly(dA–dT)]$_2$ complex shows a positive feature at 380 nm followed by a negative trend at the long-wavelength edge of the absorption (the corresponding absorption spectrum shows a tail evidencing the exciton interaction). The LD spectrum in principle contains information about the structure of this "dimer". For example, with two DAPI molecules lying in the minor groove in a head-to-tail arrangement, the low-energy component of the exciton couplet would correspond to a transition moment oriented at about 30° to the helix axis. This should give an LD that is more positive than the 45° LD of a single minor groove bound DAPI molecule. The high-energy component (to appear at shorter wavelength) would give a weak negative LD in this case. Another possibility, a stacked type of DAPI dimer (such as the dimers inferred for chromomycin (Gao & Patel, 1989) and distamycin A (Pelton & Wemmar, 1990)), would instead give a transition moment for the low-energy component which is perpendicular to the helix axis and would thus be associated with a negative LD. The high-energy component would give a strong positive LD for this case. The experimental spectrum is clearly more consistent with the latter geometry, which should then imply that quite a high number of DAPI molecules could be inserted in the minor groove, a conclusion supported by the very high maximum binding ratios observed for this drug in [poly(dA–dT)]$_2$. A recent simulation of such a binding geometry of DAPI in the minor groove shows that such a geometry is indeed possible (Mohan & Mathindra, 1991).

CONCLUSIONS

The present optical spectroscopic studies of the complexation of DAPI with polynucleotides and oligonucleotides have allowed a number of important conclusions to be drawn.

1. In AT-rich sequences, to which DAPI binds preferentially, the molecule is edgewise inserted into the minor groove with its long axis at an angle of approximately 45° to the helix axis. This binding geometry is found for very low as well as higher binding ratios.

2. The concluded geometry is in agreement with the geometry of the DAPI complex observed in the crystalline form with the Drew–Dickerson dodecamer, and the latter complex is verified to give an induced CD spectrum very similar to that of the complex with [poly(dA–dT)]$_2$ in solution.

3. Our observation of two distinct types of CD spectra, typical for the binding of DAPI to DNA and for the complex with [poly(dA–dT)]$_2$, demonstrates that the first binding mode, despite its very low apparent abundance, is not due to a specific DNA site.

4. The two binding modes could be explained in terms of an allosteric binding of DAPI to [poly(dA–dT)]$_2$ such that, when DAPI molecules bind contiguously to the AT sequence, the DNA conformation is changed to favor binding. The new conformation is responsible for the appearance of the type II induced CD spectrum of the bound DAPI chromophore. Chemometric analysis of the CD spectra of solutions with varying relative contents of the different spectroscopic species supports this model and suggests that the DNA conformation switches when at least two or three DAPI ligands are bound contiguously.

5. Results from the oligonucleotide complexes studied and evidence about the proximity of adjacent DAPI molecules at high binding ratios from exciton interactions suggest that the DAPI interactions, which are found in longer AT sequences, are of long-range nature, potentially with several base pairs separating the drug units.

APPENDIX 1

The CD spectra of DAPI bound to [poly(dA–dT)]$_2$ were analyzed by a chemometric approach (Kubista, 1990). The CD spectra of the DAPI absorbing region at 300–450 nm and mixing ratios ≤ 0.12, for which the exciton contribution to the spectra is still negligible, were normalized to 1 M total DAPI concentration and arranged as rows in an $n \times m$ matrix **A**, where $n = 12$ is the number of CD spectra used in the analysis and $m = 751$ is the number of data points for each spectrum. Since the spectral response of each component is proportional to its concentration (Beer–Lambert law), matrix **A** must equal the product **CV′**:

$$\mathbf{A} = \mathbf{CV'} \tag{A1}$$

where **V′** is an $r \times m$ matrix of the molar CD spectra of the r pure components, and **C** is an $n \times r$ matrix containing the concentrations of these components in the n samples.

The data matrix **A** is decomposed into principal components using the NIPALS algorithm (Fisher & MacKenzie, 1923):

$$\mathbf{A} = \mathbf{TP'} \tag{A2}$$

where **P′** contains the projection vectors, i.e., the principal components, as rows and **T** contains the target vectors as columns. The product **TP′** will reproduce **A**, but the **P′** matrix will not be equal to the **V′** matrix; its rows are linear combinations of the true spectra of the present components. Likewise, **T** will not equal **C** but tells only how the principal components should be combined to reproduce the measured spectra of **A**. Inspection of **P′** and **T** revealed that two components are sufficient to account for all of the spectral features in the data matrix **A**. Thus the number of independent spectral components in the samples is 2 ($r = 2$). By excluding all but the first two rows in **P′** and the first two columns in **T**, we eliminate most of the noise in the experimental data and retain only the physically relevant features (Figure 6a).

Equation A2 is one possible decomposition of **A** into a product of two matrices, but so also is eq A3, where **R** is any arbitrary nonsingular $r \times r$ matrix:

$$\mathbf{A} = (\mathbf{TR})(\mathbf{R}^{-1}\mathbf{P'}) \tag{A3}$$

The problem is now to find a matrix **R** such that

$$\mathbf{TR} = \mathbf{C} \tag{A4}$$

and

$$\mathbf{R}^{-1}\mathbf{P'} = \mathbf{V} \tag{A5}$$

For our system it is not possible to solve these equations unambiguously. However, with certain assumptions and judgement and reasonable spectra of the pure component a fair estimation can be made. Since we use only the first two

principal components, **R** is a 2 × 2 matrix:

$$\mathbf{R} = \begin{bmatrix} R_{11} & R_{12} \\ R_{21} & R_{22} \end{bmatrix} \quad \text{and} \quad \mathbf{R}^{-1} = (R_{11}R_{22} - R_{12}R_{21})^{-1}\begin{bmatrix} R_{22} & -R_{12} \\ -R_{21} & R_{11} \end{bmatrix} \tag{A6}$$

All CD spectra used in the analysis cross in an isodichroic point, which means that DAPI is quantitatively bound in these experiments. Since the spectra were scaled to unit DAPI concentration, the sum of the concentration coefficients for each sample must be equal to 1:

$$C_{1i} + C_{2i} = 1 \qquad (i = 1,n) \tag{A7}$$

Equations A4–A7 then give

$$(R_{11} + R_{12})T_{i1} + (R_{21} + R_{22})T_{i2} = 1 \tag{A8}$$

or

$$F_{11}T_{i1} + F_{12}T_{i2} = 1$$

where T_{i1} and T_{i2} are the ith elements in columns one and two, respectively, in matrix **T**. By fitting the two columns of **T** to a vector where all elements are 1, we determine $F_{11} = (R_{11} + R_{12})$ and $F_{12} = (R_{21} + R_{22})$.

The CD spectra at very low binding ratios are, within experimental error, independent of the amount of bound DAPI, and we assume that these spectra represent the spectrum of DAPI bound in the AT mode I. By letting the CD spectrum of the sample with the lowest binding ratio be the first row of matrix **A**, we have $V'_{1i} = A_{1i}$ $(i = 1, m)$ and

$$R_{22}(R_{11}R_{22} - R_{12}R_{21})^{-1}P'_{1i} - R_{12}(R_{11}R_{22} - R_{12}R_{21})^{-1}P'_{2i} = A'_{1i} \tag{A8}$$

or

$$F_{21}P'_{1i} - F_{22}P'_{2i} = A'_{1i}$$

where P'_{1i} and P'_{2i} are the ith elements in rows one and two, respectively, in matrix **P′**. By fitting the two projection vectors obtained from the NIPALS algorithm to the CD spectrum recorded at the lowest binding ratio, we determine $F_{21} = R_{22}(R_{11}R_{22} - R_{12}R_{21})^{-1}$ and $F_{22} = R_{12}(R_{11}R_{22} - R_{12}R_{21})^{-1}$.

Out of these four parameters F_{11}, F_{12}, F_{21}, and F_{22}, only three are linearly independent, and we cannot determine all four elements in the **R** matrix. However, we can use these relations to express matrix **R** with a single parameter:

$$\mathbf{R} = \begin{bmatrix} R_{11} & F_{11}-R_{11} \\ F_{12}-F_{21}(R_{11}-F_{11})/F_{22} & F_{21}(R_{11}-F_{11})/F_{22} \end{bmatrix} \tag{A9}$$

This means that for any given value of R_{11} that does not make matrix **R** singular, we can calculate a mathematically acceptable solution for **C** and **V**, where the AT mode I CD spectrum is recorded at the lowest mixing ratio and where the total concentration of DAPI in all samples sums to 1. However, not all values of R_{11} provide physically acceptable solutions, since most values of R_{11} predict negative concentrations in some of the samples. By requiring that the concentrations of the two components be nonnegative in all samples, we can considerably limit the number of solutions. Figure 6b,c shows one solution consistent with our data. Here R_{11} was tuned to give binding isotherms similar to those of random binding, where isolated bound DAPI forms one class of ligand and contiguously bound DAPI molecules form a second class. The CD spectrum of the second form, consistent with these binding isotherms (Figure 6b), has a negative feature at short wavelength which may be hard to rationalize. The spectrum is however not unphysical, and this solution cannot be ruled out on the basis of the chemometric analysis. Figure 6d shows a different solution where R_{11} was tuned to give a type II CD spectrum that is all positive and has a more traditional shape. The corresponding binding isotherms predict a larger abundance of DAPI ligands bound in mode II than expected from random occupancy, which is in agreement with an allosteric binding process that leads to a clustering of bound ligands. From the analysis we conclude that, even though our data cannot prove allosteric binding of DAPI to $[poly(dA–dT)]_2$, they are clearly consistent with such a mechanism.

APPENDIX 2

Thermodynamics of Allosteric Binding. The CD titration data are consistent with the binding model C in Figure 5, where an isolated DAPI molecule does not induce a conformational change of the DNA helix, but contiguously bound DAPI molecules do. Such a binding scenario can be rationalized by an allosteric binding model.

The thermodynamics for allosteric binding to DNA was originally described by Dattagupta et al. (1980). The DNA lattice units, the base pairs, are assumed to be in an equilibrium between two states to which the ligand binds with different affinities. These states are the standard B-form DNA (represented by white boxes) and a different state of higher energy (represented by shadowed boxes). The free DNA lattice units are then in equilibrium between these two states.

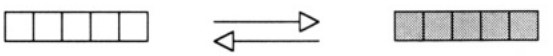

The thermodynamic parameters describing this equilibrium and ligand binding to the two states are the following:

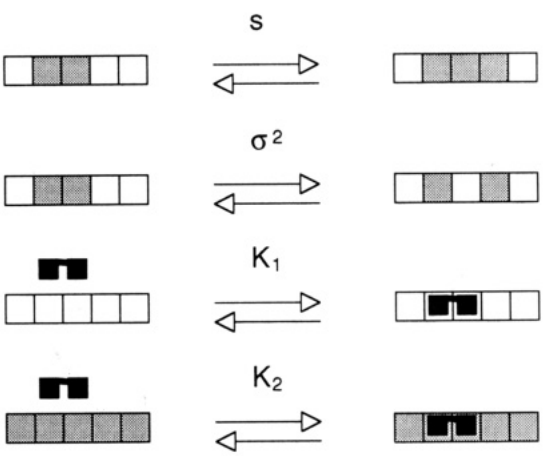

where $\Delta G_s^\circ = -RT \ln s$ is the cost in free energy when transforming 1 mol of base pairs from the B form to the high-energy state, $\Delta G_j^\circ = -RT \ln \sigma$ is the cost in free energy when creating 1 mol of junctions between lattice segments of the two states, and K_1 and K_2 are the binding constants of the ligand to the two states. In addition, a general treatment should include cooperativity interactions between the bound ligands:

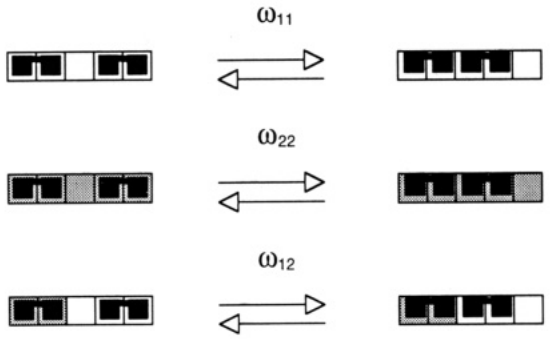

where $\Delta G_{\omega_{ij}}^{\circ} = -RT \ln \omega_{ij}$ is the change in free energy when two bound ligands, one in state i and one in state j, are brought next to each other.

In the absence of ligands, the equilibrium between the two states is shifted far to the normal B form. However, if $K_2 > K_1$, the ligands bind preferentially to the high-energy state of the lattice and may induce a conformational change. Our results demonstrate that isolated bound DAPI molecules do not induce the conformational change. Assuming a binding site of four base pairs (Portugal & Waring, 1988; Jeppesen & Nielsen, 1989), the equilibrium constant between an isolated ligand bound to B-form DNA and to a local segment of the high-energy state is $K_1/K_2 s^4 \sigma^2 > 1$. We also find that contiguously bound DAPI molecules do induce the conformational change in an AT dodecamer. This oligomer should have the capacity to bind three ligands. Since no junctions are created, $K_1^3/K_2^3 s^{12} < 1$.

Wilson et al. (1990) studied the binding of DAPI to [poly(dA–dT)]$_2$ by equilibrium dialysis and analyzed the data according to the allosteric binding model, obtaining $K_2/K_1 \approx 90$, $s \approx 0.91$, and $\sigma \approx 0.002$. Although their analysis neglected cooperative interactions between the bound ligands, these values should provide rough estimates of the thermodynamic parameters, and we calculate $K_1/K_2 s^4 \sigma^2 = 4050$ and $K_1^3/K_2^3 s^{12} = 4 \times 10^{-6}$. Although the parameters were determined at a higher ionic strength than used in our study, the calculated ratios are consistent with the inequalities deduced from our observations.

Using the thermodynamic parameters, we can calculate how many DAPI molecules should be bound contiguously to induce the conformational change. The partition constant between m contiguously bound DAPI molecules in the two states is $K_1^m/K_2^m s^{4m} \sigma^2$. For $m = 3$ this ratio equals 1.06, meaning that a lattice segment covered by three contiguously bound DAPI molecules is equally probable in either state. (Actually, the equilibrium will be shifted more to the altered state by configurations where some neighboring free bases are also in the altered state.)

The High-Energy State of DNA. Simultaneous with the appearance of a type II CD spectrum in the [poly(dA–dT)]$_2$ titration, evidencing the structural conversion of the DNA lattice, we observe an increase in the overall LD magnitude. This increase reflects a more efficient orientation of the DNA, which could be due to either a lengthening and/or a stiffening of the lattice (Nordén et al., 1992). The increase in orientation is substantial and is unlikely to be entirely a lengthening effect, and we suggest that the high-energy state is considerably stiffer than normal B-form DNA. This is in accordance with the structural change induce by netropsin (Hogan et al., 1979) and distamycin A (Dattagupta et al., 1980), where the increase in the apparent length of the DNA was estimated to be 14 Å per bound ligand, which is clearly unrealistic as an increase of the true length but rather is an indication of an increase in the persistence length of the DNA.

The structural change is related to the minor groove binding mode of DAPI and is not observed for the [poly(dG–dC)]$_2$ binding mode (Nordén et al., 1990). We note that the other ligands, netropsin and distamycin A (Hogan et al., 1979; Dattagupta et al., 1980), which induce similar conformational changes are also minor groove binders with a preference for AT regions (Zimmer & Wahnert, 1986), and we shall henceforth refer to this altered DNA form as the m form. Since these minor groove binders interact much more strongly with the m form of DNA (DAPI ~90 times (Wilson et al., 1990); distamycin ~15 times (Dattagupta et al., 1980)) despite having a similar binding geometry as when bound to standard B-DNA (Figures 1 and 2), the minor groove of the m form could be different.

Long-Range Effects Mediated through DNA Conformational Changes. The cost in having a segment of DNA in the m form is mainly due to the creation of junctions and not due as much to the energy loss of having the base pairs in the altered state. Therefore, if two segments in the m state are separated by n free bases, the system may gain in energy if the intervening free base pairs are also converted into the m state, since the energy loss in having them in the altered state is compensated for by the elimination of two junctions. The partition constant between all of the intervening base pairs in the standard B form and all in the anomalous m form is s^p/σ^2, where p is the number of free intervening base pairs. Note that the ratio only contains parameters describing properties of the DNA lattice and not properties of the ligands inducing the m state. Dattagupta et al. (1980) obtained $s \approx 0.962$–0.977 (depending on ionic strength) and $\sigma \approx 0.003$ for the conformational change induced by distamycin A. The values of the thermodynamic parameters are similar to those for the DAPI-induced conformational change (Wilson et al. (1990); see above), suggesting that the same conformational change is induced by the two drugs and that these parameters indeed are properties of the DNA lattice only. Using these values, we find that the equilibrium constant is unity for a stretch of 132–500 free base pairs (depending on which values we use) enclosed by segments of m-DNA. This means that two m-DNA segments may efficiently convert some 13–37 turns of intervening free DNA to the m form.

DAPI binds only 90 times stronger to m-DNA than to standard B-DNA ($K_2/K_1 \approx 90$), and as discussed above, three contiguously bound DAPI ligands are expected to convert B-DNA into m-DNA. However, DAPI is a small ligand, and one can imagine considerably larger K_2/K_1 ratios for other ligands. In order for a single ligand to convert DNA locally into the m form, $K_2/K_1 > s^{-n}\sigma^{-2}$, where n is the binding size. With $5 < n < 15$, the ratio K_2/K_1 must be on the order of 10^5 to bring the lattice into the m form. However, for long-range signal transmission the equilibrium constant is not the sole determinant; the rate of conversion is also important. In a possible real system a ligand may bind its binding site in standard B-DNA, but not exert its action until the DNA is converted into the m form. An effector ligand bound in its proximity may convert the DNA locally to the m form, and the structural change may transiently propagate to the first ligand and trigger its action. The rate of this process will depend on the rate and processivity of the structural conversion of the intervening sequence. In our experiments we have never observed signal changes in time. In all cases where a type II CD spectrum was observed, it was seen immediately after

sample preparation, which means that the B → m transition cannot be a very slow process.

Whether this form of signal transmission over a distance occurs in real systems, we do not know. It has not been studied very much, since there has been no way to detect this DNA structural change. However, in DAPI we have a sensitive probe for this structural change, since through its CD spectrum it will report the presence of m form induced by any other ligand.

REFERENCES

Albinsson, B., Eriksson, S., Lyng, R., & Kubista, M. (1991) *Chem. Phys. 151*, 149–157.

Barcellona, M. L., & Gratton, E. (1990) *Eur. Biophys. J. 17*, 315–323.

Barcellona, M. L., & Gratton, E. (1991) *Biophys. Chem. 40*, 223–229.

Bella, J. L., & Gosálvez, (1991) *Biotech. Histochem. 1*, 44–52.

Bernheim, A., & Miglierina, R. (1989) *Hum. Genet. 83*, 189–193.

Bierzynski, A., Boguta, G., Berens, K., & Wierzchowski, K. L. (1978) *Studia Biophys. 67*, 57–58.

Brown, R. N., & Hitchcook, P. F. (1989) *Dev. Brain Res. 50*, 123–128.

Cavatorta, P., Masotti, L., & Szabo, A. G. 91985) *Biophys. Chem. 22*, 11–16.

Chi, H., Ishibashi, Y., Shima, A., Mihara, I., & Otsuka, F. (1990) *J. Invest. Dermatol. 95*, 154–157.

Dann, O., Bergen, G., Demant, E., & Volz, G. (1971) *Liebigs Ann. Chem. 749*, 68–89.

Dattagupta, N., Hogan, M., & Chrothers, D. M. (1980) *Biochemistry 19*, 5998–6005.

Fisher, R., & MacKenzie, W. (1923) *J. Agric. Sci. 13*, 311–320.

Gao, X., & Patel, D. J. (1989) *Biochemistry 28*, 751–762.

Hajduk, S. L. (1976) *Science 191*, 858–859.

Härd, T., Fan, P., & Kearns, D. R. (1990) *Photochem. Photobiol. 51*, 77–86.

Hogan, M., Dattagupta, N., & Crothers, D. M. (1979) *Nature 278*, 521–524.

Jeppesen, C., & Nielsen, P. E. (1989) *Eur. J. Biochem. 182*, 437–444.

Kapuscinski, J., & Skozylas, B. (1978) *Nucleic Acids Res. 5*, 3775–3799.

Kapuscinski, J., & Szer, W. (1979) *Nucleic Acids Res. 6*, 3519–3534.

Kapuscinski, J., & Yanagi, K. (1979) *Nucleic Acids Res. 6*, 3535–3542.

Kubista, M. (1990) *Chemom. Intell. Lab. Syst. 7*, 273–279.

Kubista, M., Akerman, B., & Nordén, B. (1987) *Biochemistry 26*, 4545–4553.

Kubista, M., Akerman, B., & Nordén, B. (1988) *J. Phys. Chem. 92*, 2352–2356.

Kubista, M., Akerman, B., & Albinsson, B. (1989) *J. Am. Chem. Soc. 111*, 7031–7035.

Larsen, T. A., Goodsell, D. S., Cascio, D., Grzeskowiak, K., & Dickerson, R. E. (1989) *J. Biomol. Struct. Dyn. 7*, 477–491.

Lee, G. M., Thornthwaite, J. T., & Rasch, E. M. (1984) *Anal. Biochem. 137*, 221–225.

Lin, M. S., Comings, D. E., & Alfi, O. S. (1977) *Chromosoma 60*, 15–25.

Loontiens, F. G., McLaughlin, L. W., Diekmann, S., & Glegg, R. M. (1991) *Biochemistry 30*, 182–189.

Lyng, R., Rodger, A., & Nordén, B. (1991) *Biopolymers 31*, 1709–1720.

Manzini, G., Barcellona, M. L., Avitabile, M., & Quadrifoglio, F. (1983) *Nucleic Acids Res. 11*, 8861–8876.

Manzini, G., Xodo, L., Barcellona, M. L., & Quadrifoglio, F. (1985) *Nucleic Acids Res. 13*, 8955–8966.

Matsuoka, Y., & Nordén, B. (1982) *Biopolymers 21*, 2433–2452.

Matsuoka, Y., & Nordén, B. (1983) *Biopolymers 22*, 1731–1746.

McGhee, J. D., & von Hippel, P. H. (1974) *J. Mol. Biol. 86*, 469–489.

Mohan, S., & Yathindra, N. (1992) *J. Biomol. Struct. Dyn. 9*, 695–704.

Nordén, B., & Seth, S. (1985) *Appl. Spectrosc. 39*, 647–655.

Nordén, B., Eriksson, S., Kim, S. K., Kubista, M., Lyng, R., & Akerman, B. (1990) in *The Jerusalem Symposia on quantum Chemistry and Biochemistry* (Pullman, B., & Jortner, J., Eds.) Vol. 23, pp 23–41, Kluwer Academic Publishers, Dordrecht, The Netherlands.

Nordén, B., Kubista, M., & Kurucsev, T. (1992) *Q. Rev. Biophys. 25* (1), 51–170.

Pelton, J. G., & Wemmer, D. E. (1990) *J. Am. Chem. Soc. 112*, 1393–1399.

Portugal, J., & Waring, M. J. (1988) *Biochim. Biophys. Acta 949*, 158–168.

Russel, W. C., Newman, C., & Williamsson, D. H. (1975) *Nature 253*, 461–462.

Schwartz, D. C., & Koval, M. (1989) *Nature 338*, 520–521.

Szabo, A. G., Krajcarski, D. T., Cavatorta, P., Masotti, L., & Barcellona, M. L. (1986) *Photochem. Photobiol. 44*, 143–150.

Takata, K., & Hirano, H. (1990) *Acta Histochem. Cytochem. 23*, 679–683.

Tijssen, J. P. F., Beekes, H. W., & van Stevenick, J. (1982) *Biochim. Biophys. Acta 721*, 394–398.

Williamson, D. H., & Fennell, D. J. (1975) *Methods Cell Biol. 12*, 335–351.

Williamson, D. H., & Fennell, D. J. (1979) *Methods Enzymol. 56*, 728–733.

Wilson, W. D., Tanious, F. A., Barton, H. J., Strekowski, L., & Boykin, D. W. (1989) *J. Am. Chem. Soc. 111*, 5008–5010.

Wilson, W. D., Tanious, F. A., Barton, H. J., Jones, R. L., Fox, K., Wydra, R. L., & Strekowski, L. (1990) *Biochemistry 29*, 8452–8461.

Zimmer, C., & Wähnert, U. (1986) *Prog. Biophys. Mol. Biol. 47*, 31–112.